Critical Slowing Down of Cluster Algorithms for Ising Models Coupled to 2–d Gravity

Mark Bowick, Marco Falcioni,
Geoffrey Harris and Enzo Marinari(*)

Dept. of Physics and NPAC,
Syracuse University,
Syracuse, New York, 13244–1130, USA

bowick falcioni gharris@npac.syr.edu marinari@roma1.infn.it

(*) and Dipartimento di Fisica and INFN,
Università di Roma "Tor Vergata",
Viale Della Ricerca Scientifica, 00133 Roma, Italy

April 4, 1994

Abstract

We simulate single and multiple Ising models coupled to 2–d gravity using both the Swendsen-Wang and Wolff algorithms to update the spins. We study the integrated autocorrelation time and find that there is considerable critical slowing down, particularly in the magnetization. We argue that this is primarily due to the local nature of the dynamical triangulation algorithm and to the generation of a distribution of baby universes which inhibits cluster growth.

Considerable work has been devoted to the study of the performance of cluster algorithms in reducing the critical slowing down of many statistical models. The Swendsen-Wang [1] and the Wolff [2] algorithms have proven very effective in beating the critical slowing down (CSD) exhibited by these models when simulated with a standard Metropolis [3] update. Reviews on cluster algorithms and CSD may be found on refs. [4]. In recent years, the numerical study of Potts models coupled to 2–d gravity has received much attention [5, 6, 7, 8], aided as well by increased analytical understanding of these models [9]. Cluster algorithms have proved useful in saving computational effort on the update of the Potts variables. The present study is motivated by the fact that there is little understanding of the actual extent of the improvement achieved in these simulations. It is worthwhile, therefore, to measure CSD in the case of simple Ising spins coupled to a dynamical lattice in order to quantify the performance of cluster algorithms. We find that there is considerable CSD, especially in the magnetization, and we relate this to the dynamics of cluster formation on a random lattice.

We shall consider a model in which $n_{\rm s}$ Ising spins are attached to the vertices of triangulations. The triangulations are characterized by their adjacency matrix $C_{\rm ij}$, which equals 1 if i and j are neighbors and vanishes otherwise. $C_{\rm ij}$ is the discrete analogue of the world-sheet metric $g_{\rm ij}$. We shall restrict ourselves to the set of triangulations with N vertices $\mathcal{T}_N$ containing only loops of length 3 or greater and vertices of coordination number of at least 3. The triangulation has a fixed toroidal topology. We simulate a theory determined by the partition function

$$Z_N = \sum_{T\in\mathcal{T}_N} \sum_{\sigma_{\rm i}=\pm 1} \exp\left(-\beta \sum_{\alpha=1}^{n_{\rm s}} \sum_{\rm i,j=1}^{N} C_{\rm ij}(T)\sigma_{\rm i}^{\alpha}\sigma_{\rm j}^{\alpha}\right), \tag{1}$$

where α labels the spin species. In refs. [10, 11] we investigated in detail this model for the cases $n_{\rm s} = 1$ and 2. We measured spin susceptibility and percolation critical exponents using finite-size scaling and showed that logarithmic corrections to scaling were essential for agreement between the measured and theoretical exponents. In this paper, we deal with the cases $n_{\rm s} = 1$, 2 and 3, concentrating on the issue of CSD and its origin.

The standard way of implementing the partition function (1) via a Monte Carlo simulation is to use the Swendsen-Wang (SW) or Wolff cluster algorithm to update the spin variables and to use the "link flip" [12] to simulate the sum over all triangulations. To implement a SW update one first divides all of the spins into Fortuin-Kasteleyn (FK) clusters [13]. These

clusters of bonded spins are created by introducing bonds between same sign spins with probability $p = 1 - \exp(-2\beta)$. Then, one flips all clusters with probability one-half. The Wolff algorithm consists of randomly choosing a spin, constructing a FK cluster around it and flipping the cluster with probability one. To compare the autocorrelation times of the SW and Wolff algorithms one should define the Wolff update so that both algorithms require comparable CPU time. For this reason we choose a Wolff update to consist of consecutive flips of FK clusters that reverse the sign of at least 40% of the spins. One alternative to this would be to scale the correlation times using the average cluster size [14]. Each spin update precedes a mesh update, in which we attempt to flip $3N$ randomly chosen links, N being the number of vertices of the triangulation. Our implementation ensures that the relative number of mesh and spin updates is roughly equivalent.

The observables that we analyzed are the energy density, the magnetization density, the susceptibility (namely the magnetization squared) and the average value of $|q-6|$, where q is the coordination number of a vertex of the triangulation. In some of the simulations that employed SW updates, we also measured the mean size of pure percolation and FK clusters. The mean FK cluster size $\mathcal{S}_{\rm FK}$ is given by the quantities $\langle s\rangle_{\rm Wolff}$ and $\langle s^2\rangle_{\rm SW}/\langle s\rangle_{\rm SW}$; s denotes the number of sites constituting a cluster and averages are taken over the distribution of clusters built in the Wolff and SW algorithms respectively. The magnetic Ising observables are directly related to the structure of these clusters [15]. In particular, for $\beta \leq \beta_c$, $\mathcal{S}_{\rm FK}$ is equal to the susceptibility, defined as

$$\chi = \frac{\beta}{N}\langle M^2\rangle, \tag{2}$$

where M denotes the average magnetization density. Actually, this alternative definition of χ is used as a reduced variance estimator [16].

Before moving on to present our results, we discuss how we estimated the autocorrelation times. It is known [17] that the following relation holds between the estimators of the naive and true variance of an observable O;

$$\mathrm{Var}(O)_{\rm true} \simeq 2\ \tau_{\rm int}\ \mathrm{Var}(O)_{\rm naive}. \tag{3}$$

For a subset of our data, we also directly measured the autocorrelation function and through standard methods [17] computed $\tau_{\rm int}$. We verified (see also [18]) that both of the above techniques gave consistent values of $\tau_{\rm int}$. The variances of the observables were extracted

from the raw data using the *binning* method. To extract the dynamic exponent, we fit the data according to the scaling ansatz

$$\tau_{\rm int} \propto N^{z/d_H}. \tag{4}$$

It is difficult to estimate the linear size of random triangulations. Therefore, we shall leave explicit the dependence of the exponent upon the intrinsic Hausdorff dimension d_H of the triangulation and fit our data using the total area N. The values of z/d_H were extracted from the auto-correlation data using a log-log regression fit, excluding from the fit the results for the smaller volumes, since they are affected the most by finite-size effects. The values of χ^2 per degree of freedom were always of order one. In the case of the magnetization for the $n_{\rm s} = 2$ and 3 models, Wolff algorithm, we extracted the exponent using only the two largest lattices, since there are larger finite-size effects.

	z/d_H		
Model	Metropolis	SW	Wolff
$n_{\rm s} = 1$	$.85 \pm .06$	$.58 \pm .05$	$.54 \pm .05$
$n_{\rm s} = 2^{(*)}$	$.95 \pm .05$	$.62 \pm .06$	$.58 \pm .09$
$n_{\rm s} = 3^{(*)}$	$.9 \pm .1$	$.49 \pm .08$	$.55 \pm .1$

Table 1: Critical exponent z/d_H for the Magnetization from fits. (*) These numbers are not reliable; we discuss this point in the text.

We present results for three different models, $n_{\rm s} = 1$, 2 and 3. Each model was simulated with the SW, Wolff and Metropolis algorithms. The $n_{\rm s} = 1$ model was simulated at the critical value of β, which is known analytically [10]. For the other models we chose the β value by looking at the peak of the susceptibility and the intersection of the Binder's cumulant [19] curves [10]. Each simulation (model and algorithm) was run at four or five values of N (512, 1024, 2048, 4096 and 8192 in the $n_{\rm s} = 1$ model) and each consisted of 10^5 thermalization sweeps and 3–5×10^5 measurement sweeps. Measurements were taken every sweep.

From the analysis presented in figures 1, 2, 3 and 4 and tables 1 and 2, we deduce the following:

	z/d_H		
Model	Metropolis	SW	Wolff
$n_s = 1$	$.62 \pm .03$	$.057 \pm .005$	$.04 \pm .03$
$n_s = 2$	$.35 \pm .1$	$.08 \pm .02$	$.17 \pm .08$
$n_s = 3$	$.5 \pm .1$	$.05 \pm .04$	$.37 \pm .08$

Table 2: Critical exponent z/d_H for the Energy from fits.

1. There is considerable critical slowing down in these models. Figure 1 shows the improvement gained by the use of cluster algorithms—the autocorrelation times *and* the dynamic exponent are significantly lower than the corresponding Metropolis values.

2. In all cases, the magnetization is the observable that suffers most from critical slowing down. This behavior is quite different from that of the Ising model on a regular lattice, where the energy exhibits CSD equal to or greater than that of the magnetization [20]. In our simulations the observable $|q-6|$ did not show any significant CSD.

3. The SW and Wolff algorithms have similar performance within the statistical accuracy of our data. On the smaller lattices the Wolff algorithm is somewhat more efficient than SW, but this advantage is a finite size artifact since it disappears on the larger lattices. For 2–d Ising models on flat and Poissonian lattices these algorithms exhibit roughly comparable performance [18, 20]. In the 3–d case, the Wolff algorithm is much more efficient. It seems that the relative performance of SW and Wolff algorithms depends on the dimensionality of the lattice.

4. It is hard to determine differences in the degree of CSD between one and two Ising models coupled to gravity, given our statistics. In [10] we found, in fact, that the numerically measured behavior of the one and two species models is very similar. This, however, is a consequence of logarithmic corrections [21] in the two-species model. One might suspect that the scaling law for τ in this model incorporates logarithms as well. On much larger lattices where logarithmic behavior is distinguishable from small power law scaling, the effective CSD might be considerably different in the two generation, as compared to one generation, case. This situation is similar to that of the 2–d 4–state Potts model. Here, Li and Sokal [22] have shown that measurements of z, obtained

using the ansatz (4), violate rigorous bounds. They suggest that these measurements of z are not correct because the fits to τ fail to take into account logarithmic corrections. For the $n_s = 3$ model the situation is worse; the corrections to scaling of (4) may be even larger. In this case, there are no theoretical arguments that predict the form of these corrections. Therefore, we anticipate that the numbers we have quoted for z/d_H differ considerably from the correct asymptotic values in the $n_s = 2$ and 3 cases. To give a sense of the magnitude of the corrections to scaling we note that on similar size lattices, the estimate of $\gamma/\nu d_H$ differs by about 3% from its asymptotic value in the $n_s = 1$ case and by almost 50% in the $n_s = 2$ case [10].

The presence of CSD in these models should not be a surprise, since the triangulation is updated locally. In this context, it is relevant to briefly recall the results of a similar analysis [11] in which percolation clusters were studied on random triangulations without matter (pure gravity). The meshes were updated locally; all link flips that did not lead to degenerate triangulations were allowed. It has been shown that these random triangulations are characterized by a scaling distribution of baby universes [23]. The formation of clusters is quite sensitive to the presence of the bottlenecks (see fig. 5), which inhibit cluster growth into and out of baby universes. Since this structure of baby universes is slow to decorrelate under the local link-flip updates, we expect that the mean percolation cluster sizes will be afflicted by critical slowing down. In the case of pure gravity, the mean size of percolation clusters built on these triangulations in fact exhibits critical slowing down of magnitude $z/d_H = .70(2)$. We also constructed percolation clusters in the Ising simulations that used SW spin updates. We observed, in this case, a similar CSD of the world-sheet geometry; z/d_H for the mean size of pure percolation clusters was measured to be .74(6).

We now argue that the critical slowing down in the gravity sector should lead to considerable CSD for magnetic observables. For one would expect that baby universes should trap FK clusters as well as pure percolation clusters. As said before, for an Ising model simulated on an arbitrary random triangulation, the mean FK cluster size equals the average magnetic susceptibility. The value of the magnetization is thus clearly sensitive to those features of the geometry that strongly affect the FK cluster size. This coupling transfers critical slowing down to the magnetic sector. Some evidence in support of this argument follows from our measurements of the mean size of the FK clusters built to perform SW updates. This observable exhibited a value of z/d_H of .52(6).

The efficiency of cluster algorithms is also typically affected by the distribution of cluster sizes. If the clusters are too small, flipping them will fail to decorrelate distant spins. If one cluster fills most of the lattice, successive flips will essentially cancel each other out. Indeed FK clusters, on average, are much smaller in the dynamical case than in the case of a fixed flat lattice. Their mean size is determined by the exponent $\gamma/\nu d_H$; $\mathcal{S}_{\rm FK} \sim N^{\gamma/\nu d_H}$. For flat lattices, $\gamma/\nu d_H = 7/8$. It is $2/3$ for the $n_{\rm s} = 1$ Ising model, which is quite close to the value for the 3–d Ising model[1].

It is difficult to determine directly whether the autocorrelation times are influenced primarily by the slow decorrelation of the world-sheet geometry or the effects of the smaller cluster sizes. The argument, however, that CSD arises from updates of the geometry applies only to magnetic observables, and not to the energy density. Since the CSD we observe is greater for the magnetization, it seems likely that the slow decorrelation of the world-sheet geometry is the primary mechanism responsible for CSD.

Acknowledgments

This work has been done with NPAC (Northeast Parallel Architectures Center) and CASE computing facilities. We would like to thank John Apostolakis, Simon Catterall and Paul Coddington for helpful correspondence and conversations. MF wishes to thank G. Thorleifsson for stimulating discussions. The research of MB was supported by the Department of Energy Outstanding Junior Investigator Grant DOE DE–FG02–85ER40231, that of MF by funds from NPAC and that of GH by research funds from Syracuse University.

References

[1] R. H. Swendsen and J.-S. Wang, Phys. Rev. Lett. 58 (1987) 86.

[2] U. Wolff, Phys. Rev. Lett. 62 (1989) 361.

[1] Simulations of the 3–d Ising model with cluster algorithms suffer noticeable critical slowing down, though still rather modest compared to the CSD observed here. In the flat 3–d case the energy is the observable showing the greater CSD.

[3] N. Metropolis, A. W. Rosenbluth, M. N. Rosenbluth, A. H. Teller and E. Teller, J. of Chem. Phys. 21 (1953) 1087.

[4] A. D. Sokal, Computer Simulation Studies in Condensed Matter Physics: Recent Developments, eds. D. P. Landau, K. K. Mon and H. -B. Schüttler (Springer-Verlag, Berlin-Heidelberg, 1988).
U. Wolff, Proc. of the 1989 Symposium on Lattice Field Theory, Capri, Nucl. Phys. B (Proc. Suppl.) 17 (1990) 93.

[5] J. Jurkeiwicz, A. Krzywicki, B. Petersson, B. Söderberg, Phys. Lett. B213 (1988) 511.

[6] C. Baillie and D. Johnston, Mod. Phys. Lett. A7 (1992) 1519; Phys. Lett. B286 (1992) 277.

[7] S. M. Catterall, J. B. Kogut and R. L. Renken, Phys. Rev. D45 (1992) 2957; Phys. Lett. B292 (1992) 277.

[8] J Ambjørn, B. Durhuus, T. Jónsson and G. Thorleifsson, Nucl. Phys. B398 (1993) 568.

[9] V.A. Kazakov, Phys. Lett. A119 (1986) 140.
D. V. Boulatov and V. A. Kazakov, Phys. Lett. B186 (1987) 379.

[10] M. Bowick, M. Falcioni, G. Harris and E. Marinari, Two Ising Models Coupled to 2–Dimensional Gravity, Syracuse Univ. preprint SU-HEP-93–4241–556 and hep-th/9310136.

[11] G. Harris, Percolation on Strings and the Cover-up of the c = 1 Disaster, Syracuse Univ. preprint SU-HEP-93–4241–555 and hep-th/9310137.

[12] D. Boulatov, V. Kazakov, I. Kostov and A. A. Migdal. Phys. Lett. B157 (1985) 295.

[13] C. M. Fortuin and P. W. Kasteleyn, Physica 57 (1972) 536.

[14] U. Wolff, Phys. Lett. B228 (1989) 379.

[15] D. Stauffer and A. Aharony, Introduction to Percolation Theory, Taylor and Francis, London, U.K., 1992.

[16] M. Sweeny, Phys. Rev. B27 (1983) 4445.

[17] A. D. Sokal, Monte Carlo Methods in Statistical Mechanics: Foundations and Algorithms, NYU preprint based on the lectures at the Troisième Cycle de la Physique en Suisse Romande, June 1989.

[18] W. Janke, M. Katoot, and R. Villanova, preprint UAB-FT-318 and hep-lat/9310025.

[19] K. Binder, Z. Phys. B43 (1981) 119.

[20] C. F. Baillie and P. D. Coddington, Phys. Rev. B43 (1991) 10617.

[21] I. Klebanov, String Theory in Two-Dimensions, in Proc. of the Trieste School on String Theory and Quantum Gravity '91, hep-th/9108019.

[22] X.-J. Li and A. D. Sokal, Phys. Rev. Lett. 63 (1989) 827.

[23] S. Jain and S. Mathur, Phys. Lett. B286 (1992) 239; J. Ambjørn, S. Jain and G. Thorleifsson, Phys. Lett. B307 (1993) 34.

Figure Captions

Figure 1: Comparison of the integrated autocorrelation times for the magnetization in the $n_s = 1$ model. The dashed lines are log-log regression fits.

Figure 2: Comparison of the integrated autocorrelation times for the energy in the $n_s = 1$ model.

Figure 3: Comparison of the integrated autocorrelation times for the magnetization in the $n_s = 2$ model. We excluded smaller volume points from the fits.

Figure 4: Comparison of the integrated autocorrelation times for the energy in the $n_s = 2$ model.

Figure 5: Schematic representation of a baby universe.

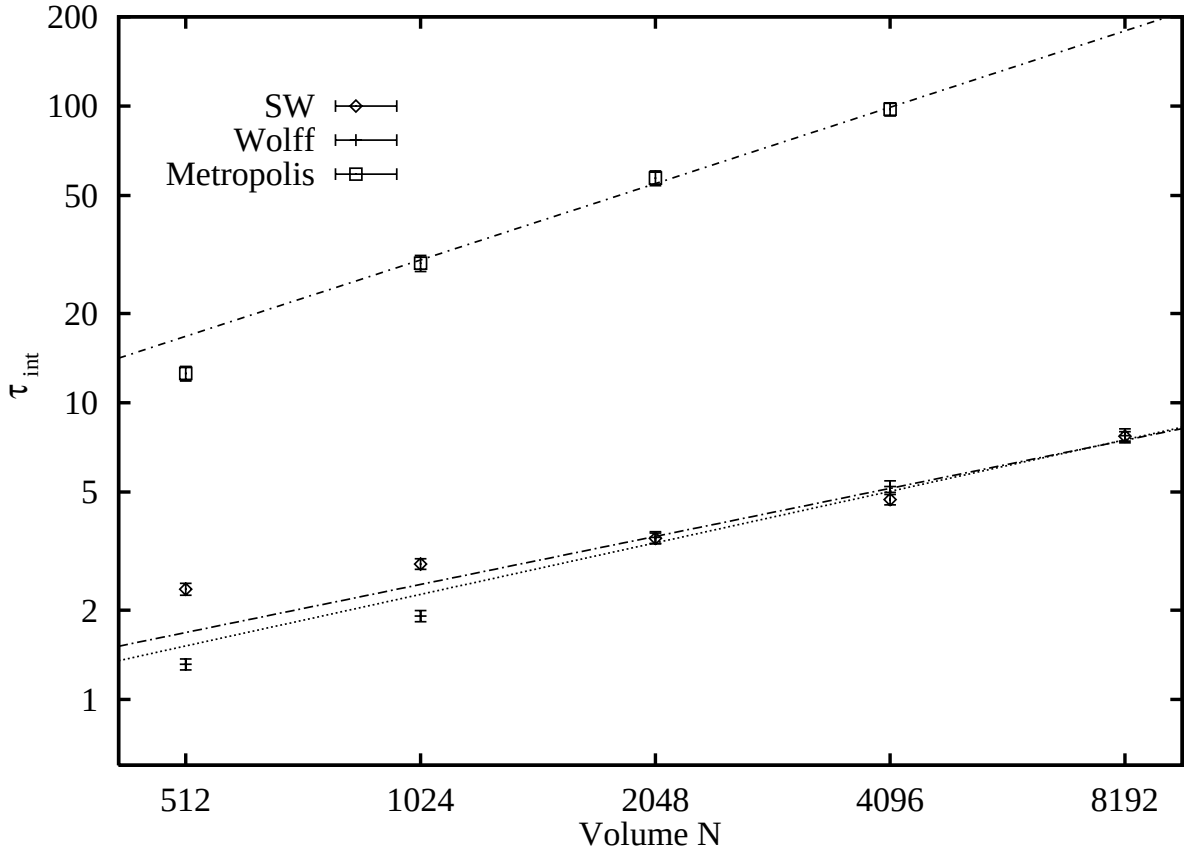
200
100
50
20
10
5
2
1
SW
Wolff
Metropolis
τ int
512
1024
2048
4096
8192
Volume N

Figure 1:

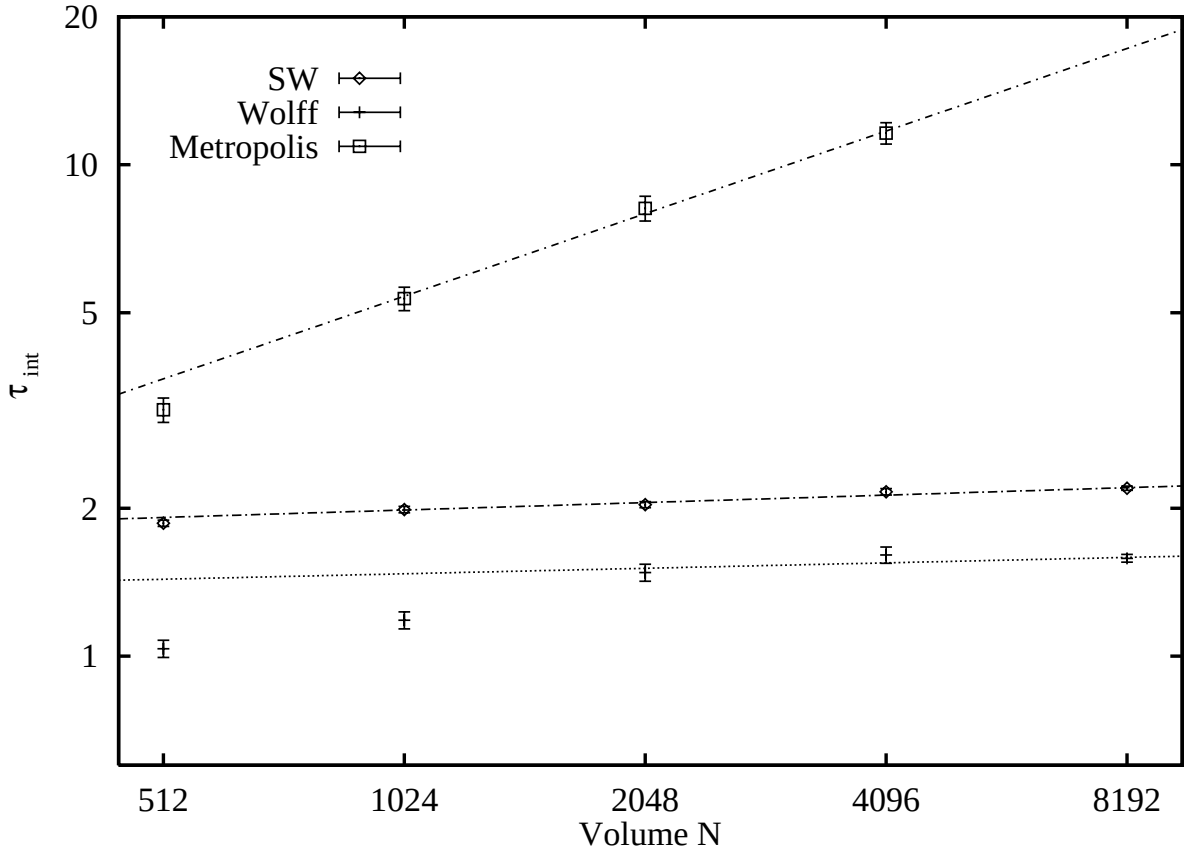
20
10
5
2
1
SW
Wolff
Metropolis
τ int
512
1024
2048
4096
8192
Volume N

Figure 2:

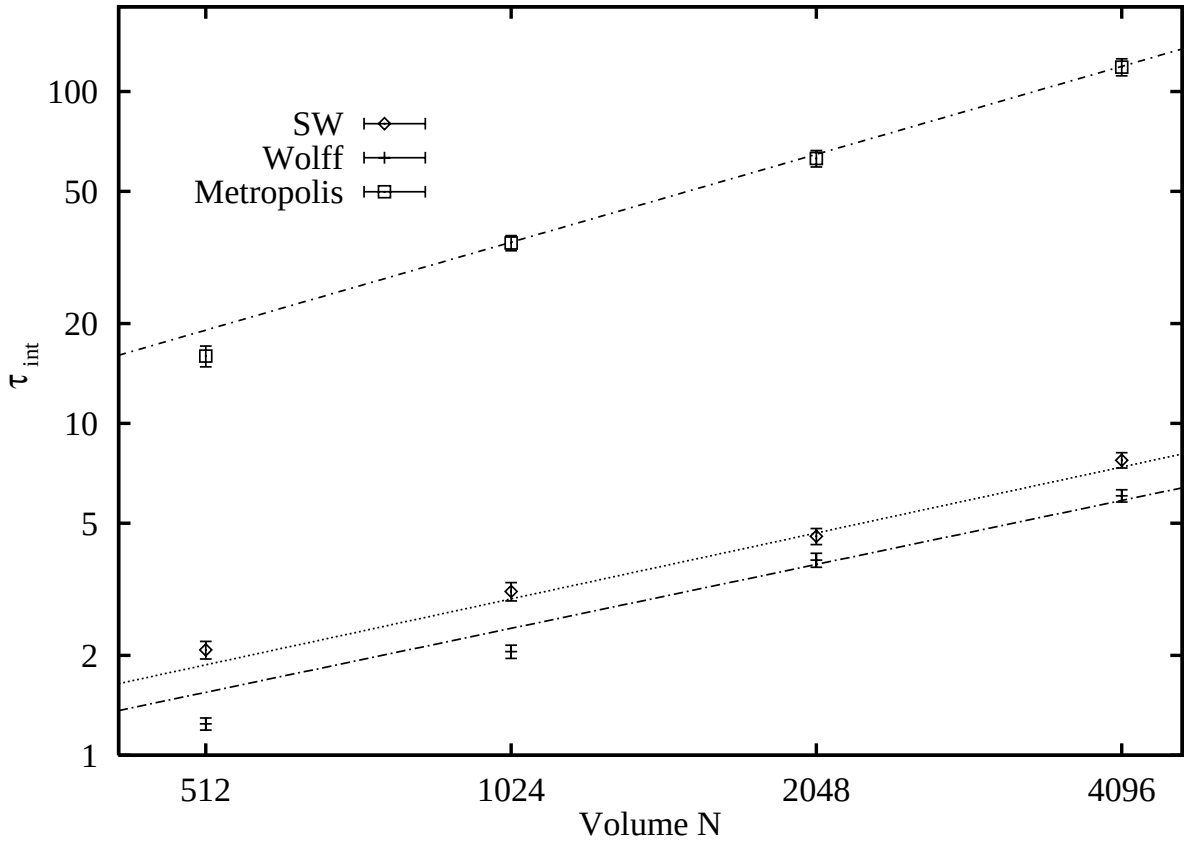
SW
Wolff
Metropolis
100
50
20
10
5
2
1
τ int
512
1024
2048
4096
Volume N

Figure 3:

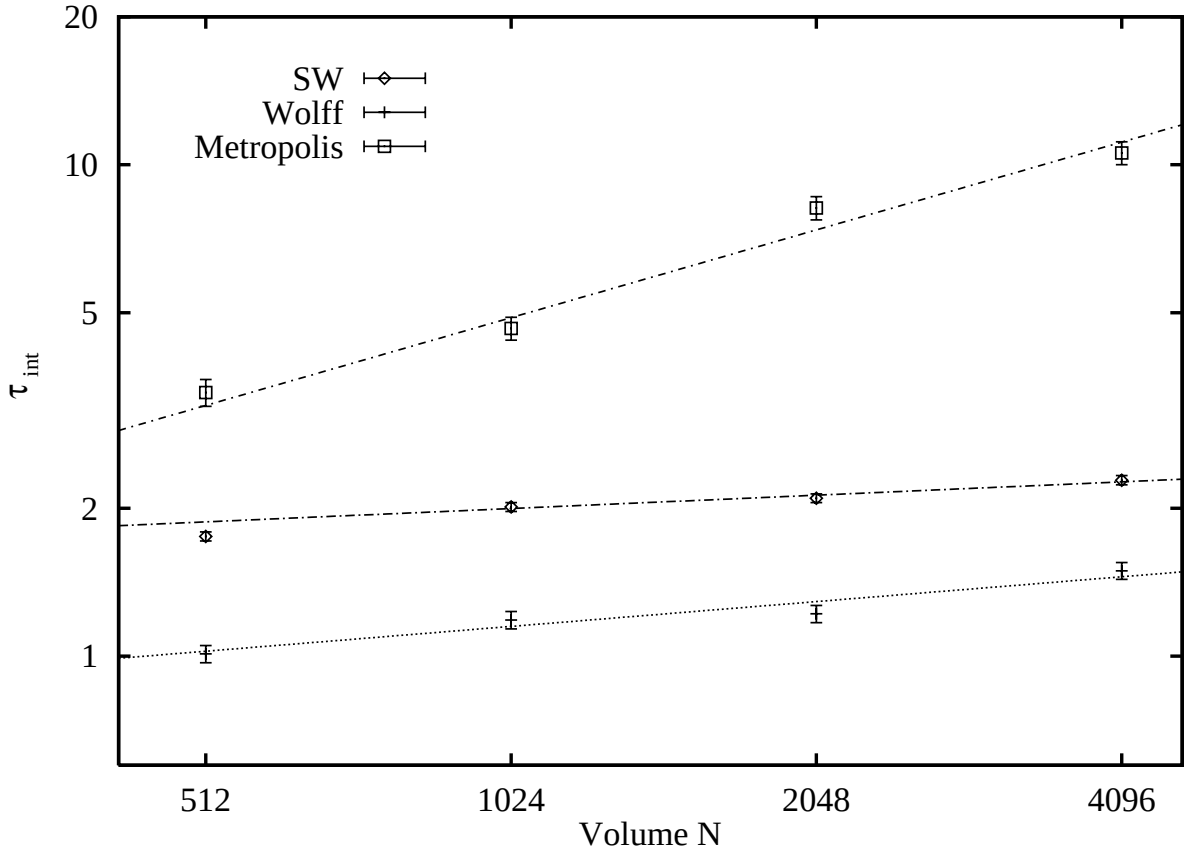
20
10
5
2
1
SW
Wolff
Metropolis
τ int
512
1024
2048
4096
Volume N

Figure 4:

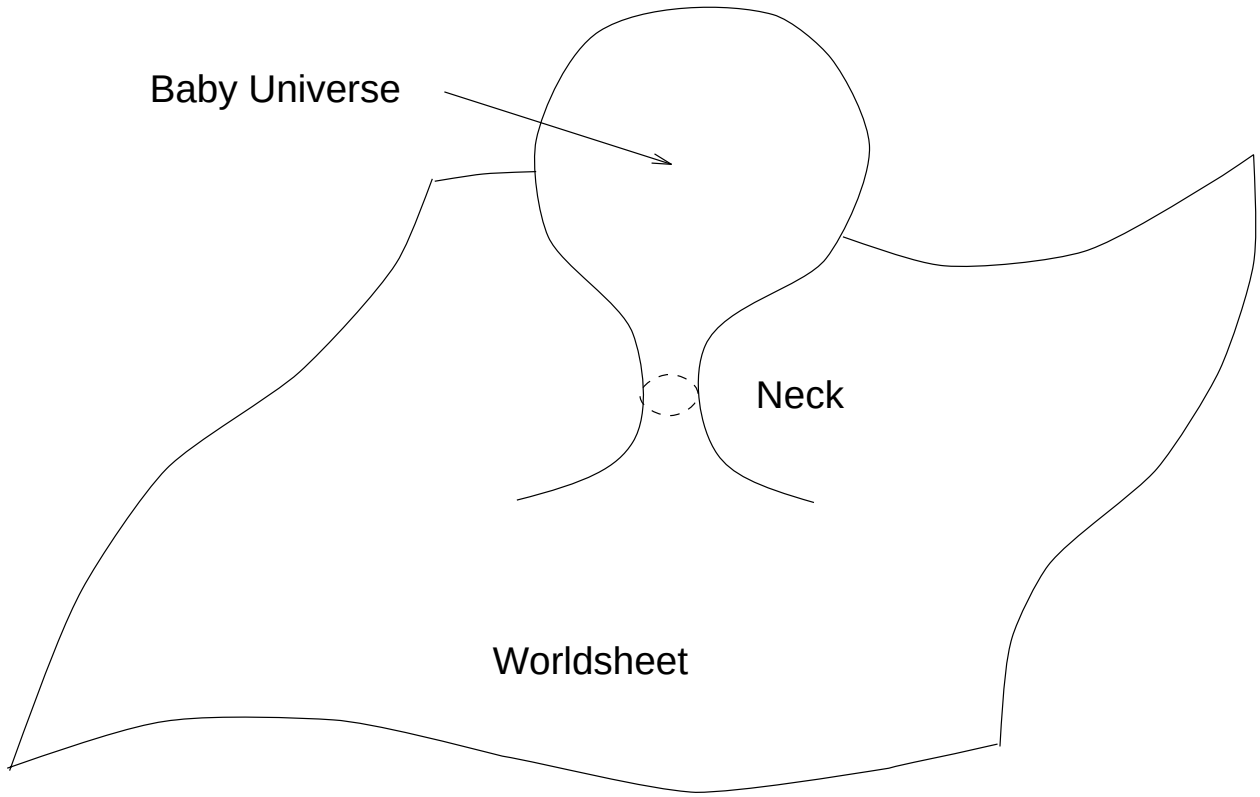

Figure 5: